

COD Criterion to Assess High Temperature Biaxial Low Cycle Fatigue

Naomi Hamada

Hiroshima-Denki Institute of Technology, Hiroshima, Japan.

Masao Sakane and Masateru Ohnami

Faculty of Science and Engineering, Ritsumeikan University, Kyoto, Japan.

Third International Conference on Biaxial/Multiaxial Fatigue, April 3-6, 1989
Stuttgart, FRG

1. Introduction

Studies of multiaxial low cycle fatigue are an important problem from a view point of design criterion of practical components since they suffer more or less biaxial/multiaxial loadings. In the previous papers[1-9], the authors have discussed the multiaxial fatigue criterion at high temperatures and have found that classical parameters such as Mises' parameter are not appropriate, but the COD criterion [2,4,5] and γ plane theory [10,11] are a proper parameter for the biaxial low cycle fatigue data correlation.

This paper derives the stress/strain multiaxial fatigue parameters in more simplified form and also discusses the applicability of the COD parameters to high temperature multiaxial fatigue data.

2. COD Criterion

2.1 High Temperature Fatigue Life in Biaxial Stress States.

Before deriving the COD parameter, we will discuss the correlation of the biaxial fatigue data with the classical parameters. The specimen used was a thin walled SUS304 austenitic stainless steel cylinder solution treated at 1373K, whose inner diameter is 9mm, outer diameter 11mm and gage length 20mm. The specimen used for the stress controlled test has a center notch of 1mm-diameter in order to observe the crack initiation and extension, but that used for the strain controlled test has no notch. Test apparatus was an electoro-hydraulic

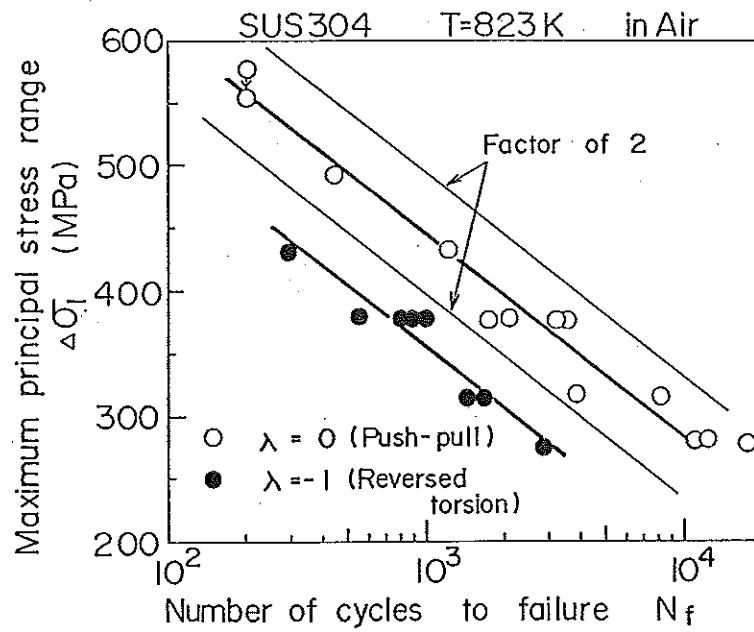
servo machine which can apply an axial load in combination with a torsional load in any loading wave shape.

Figure 1 [5,7] shows the correlation of the stress controlled biaxial fatigue data with (a) the maximum principal stress and (b) the Mises' stress, and the strain controlled fatigue data with (c) the maximum principal strain and (d) the Mises' strain. On the stress base, the maximum principal stress correlates the reversed torsion data ($\lambda=-1$) below the push-pull data ($\lambda=0$), while the Mises' stress reverses the trend of the correlation. On the strain base, the reversed torsion data ($\phi=-1$) are arranged conservatively and are just outside a factor of two scatter band. The Mises' strain enlarges the scatter of the data than the maximum principal strain. In these figures, λ is the ratio of the minimum principal stress to the maximum one and ϕ is that of the maximum principal strain to the minimum one. The data correlation with the strain parameters yields a smaller scatter of the data in comparison with the stress parameters.

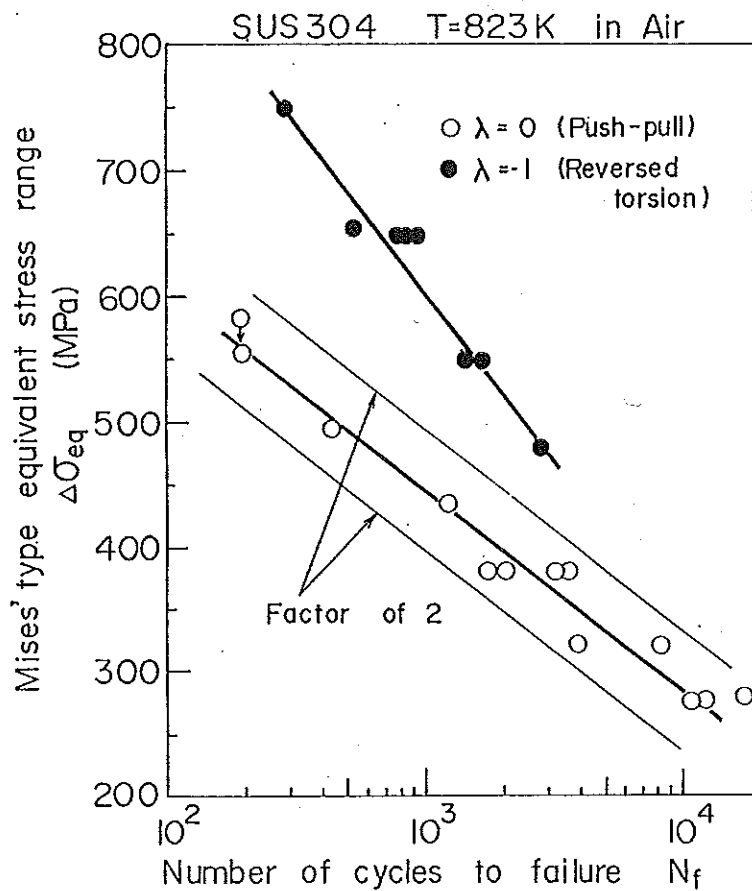
The above discussion cleared that the classical parameters, such as the maximum principal and Mises' parameters are not effective to the multiaxial fatigue data correlation. In the next section, we will discuss the cause of the ineffective data correlation from crack behavior.

2.2 Effect of Parallel Stress on Fatigue Crack Propagation.

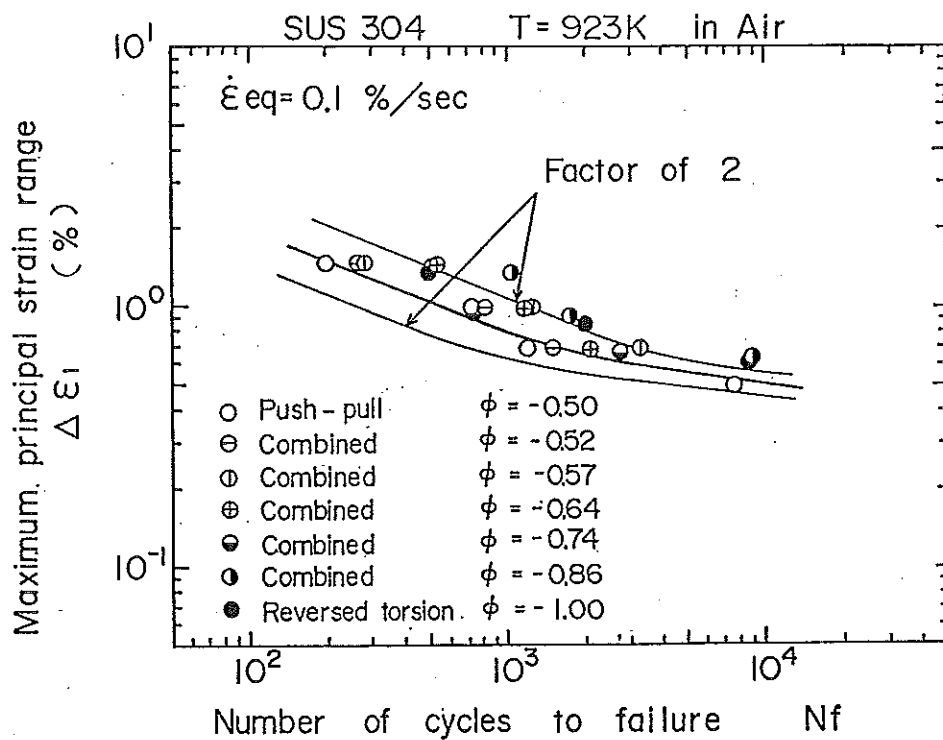
Now, we discuss the effect of parallel stress on fatigue crack propagation and clear why the reversed arrangement occurs between Fig.1(a) and Fig.1(b). The relation between crack direction and applied stress is schematically shown in Fig.2, where (a) is the push-pull test and (b) the reversed torsion test. Since the crack propagated in the normal direction to the maximum principal stress in both the tests, only the difference is the application of the parallel stress to the crack. There exists no parallel stress in the push-pull test but exists the parallel stress of which sign and amplitude are respectively opposite and same to the normal in the principal stress controlled test.



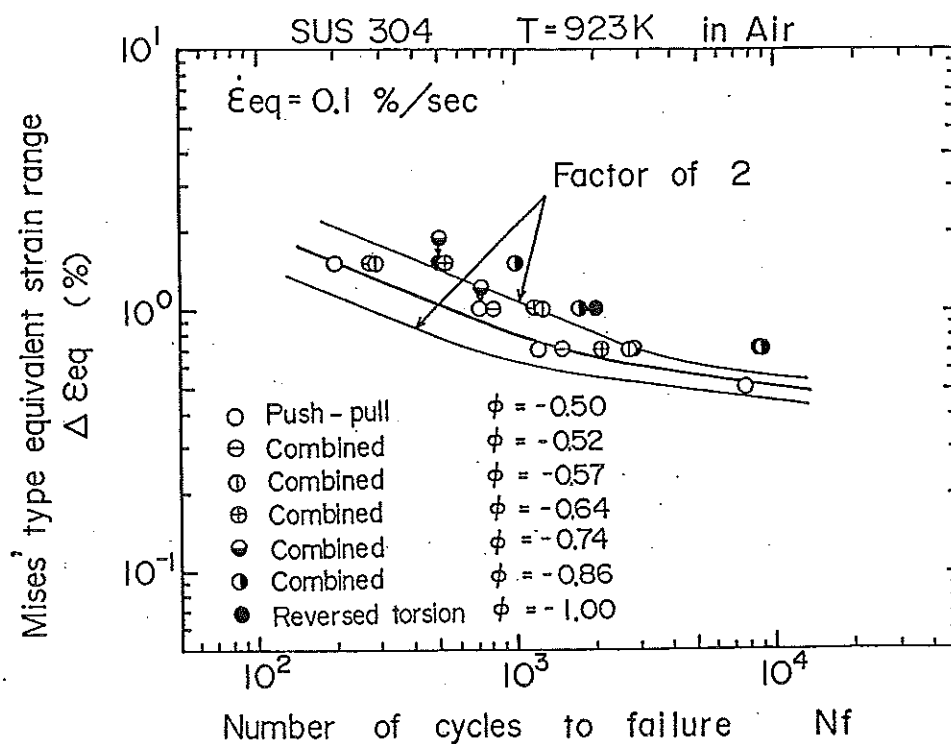
(a) Maximum principal stress



(b) Mises' equivalent stress



(c) Maximum principal strain



(d) Mises' equivalent strain

Fig.1 Correlation of biaxial fatigue life with classical parameters

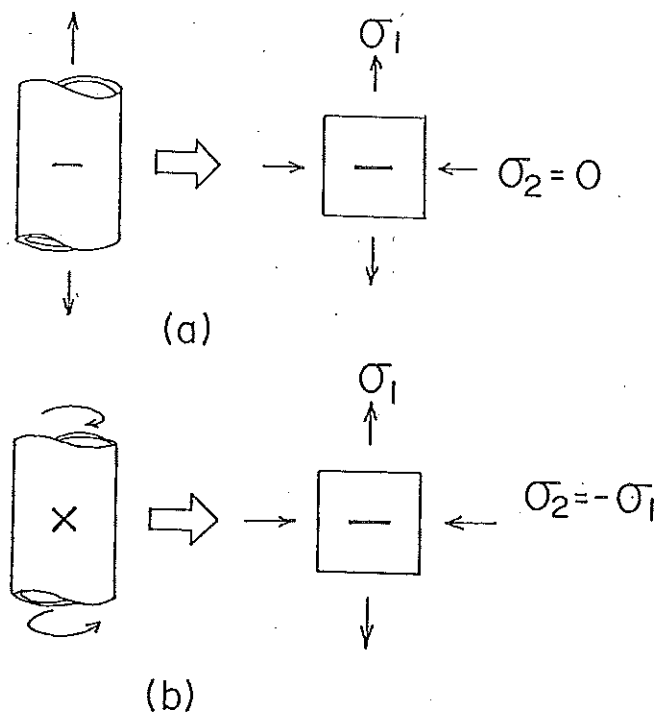


Fig.2 Schematic figure showing relationship between the crack direction and applied stress in the stress controlled push-pull and reversed torsion tests.

Figure 3 [5] shows the experimental relation between crack propagation rate, dl/dN , and crack length, l . The crack propagation rate in the reversed torsion test is larger than that in the push-pull test at the same crack length. This indicates that the compressive stress parallel to fatigue crack accelerates the crack propagation rate so that the maximum principal stress locates the reversed torsion data unconservatively because it does not take account of the effect of parallel stress.

On the other hand, since the Mises' stress, σ_{eq} , is equated as $\sigma_{eq} = (\sigma_1^2 - \sigma_1\sigma_2 + \sigma_2^2)^{1/2}$ with σ_1 and σ_2 , it estimates the contribution of parallel stress same as σ_1 . This is the excessive estimate of σ_2 than the actual. Thus, the Mises' stress correlates the reversed torsion data conservatively. In conclusion, if we can find a parameter which estimates the contribution of the parallel stress properly, the parameter will be a good measure to correlate the multiaxial fatigue life.

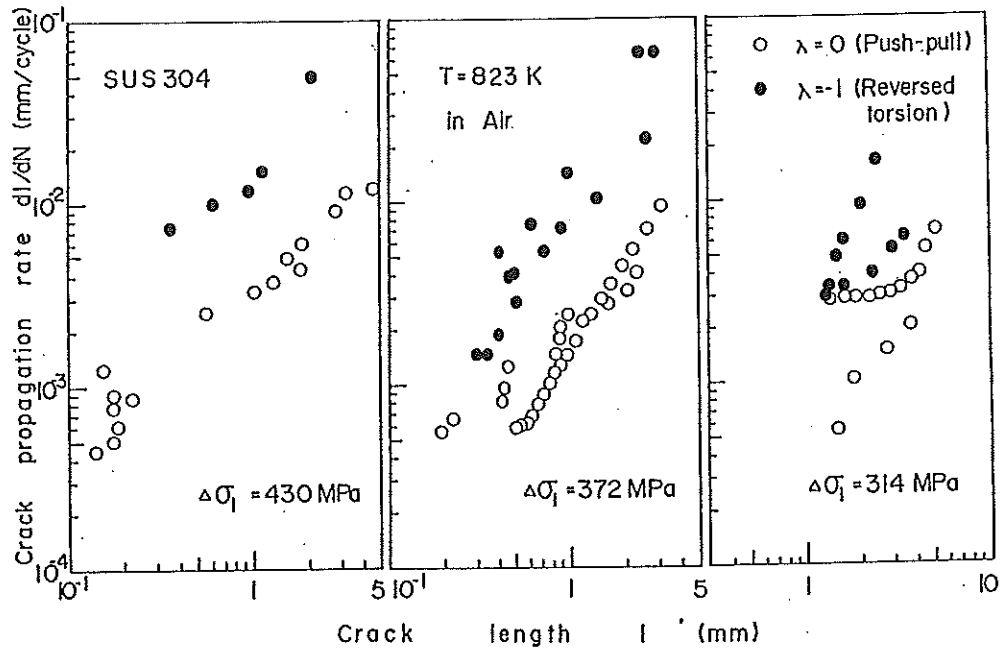


Fig.3 Experimental relationship between crack propagation rate and crack length.

The above discussion is on the stress controlled fatigue. As for the strain controlled fatigue shown in Figs.1(c) and (d), the same argument holds if we discuss the strain controlled fatigue from the viewpoint of applied stress. The detailed discussion on the strain controlled fatigue has been published elsewhere [2].

Figure 4 [5] shows the rearrangement of the crack propagation rate with crack opening displacement, COD, measured in experiment. Crack opening displacement correlates successfully the crack propagation rate regardless of the stress level and principal stress ratio. Thus, if we can express the COD by a simple equation with the applied stresses the equation will be a good comparison parameter for arranging the biaxial fatigue data. We will formulate the equation from the FEM analysis.

3. Derivation of COD Parameter

Figure 5 [4] shows a result of the elastic-plastic FEM analysis for a center cracked plate in static tension. The figure shows the relation between

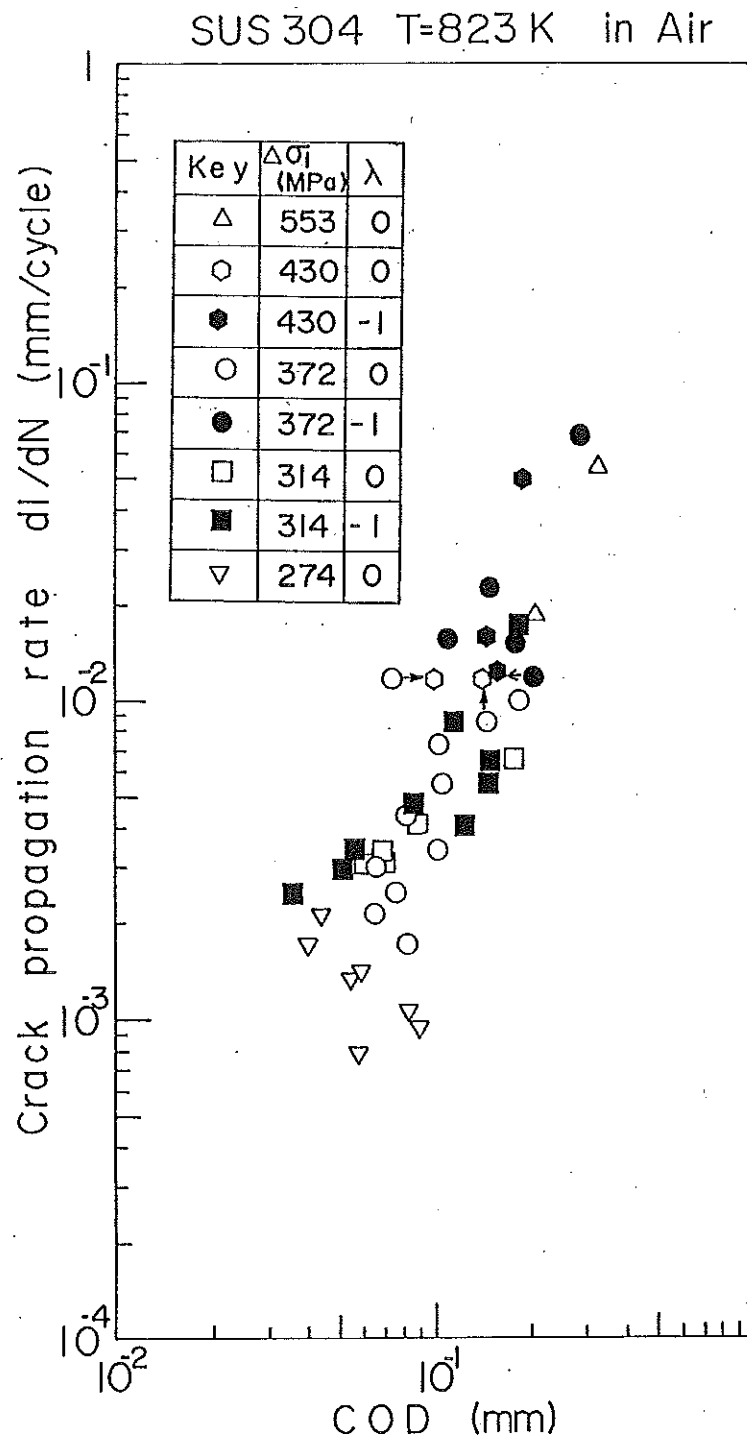


Fig.4 Experimental relationship between crack propagation rate and crack opening displacement.

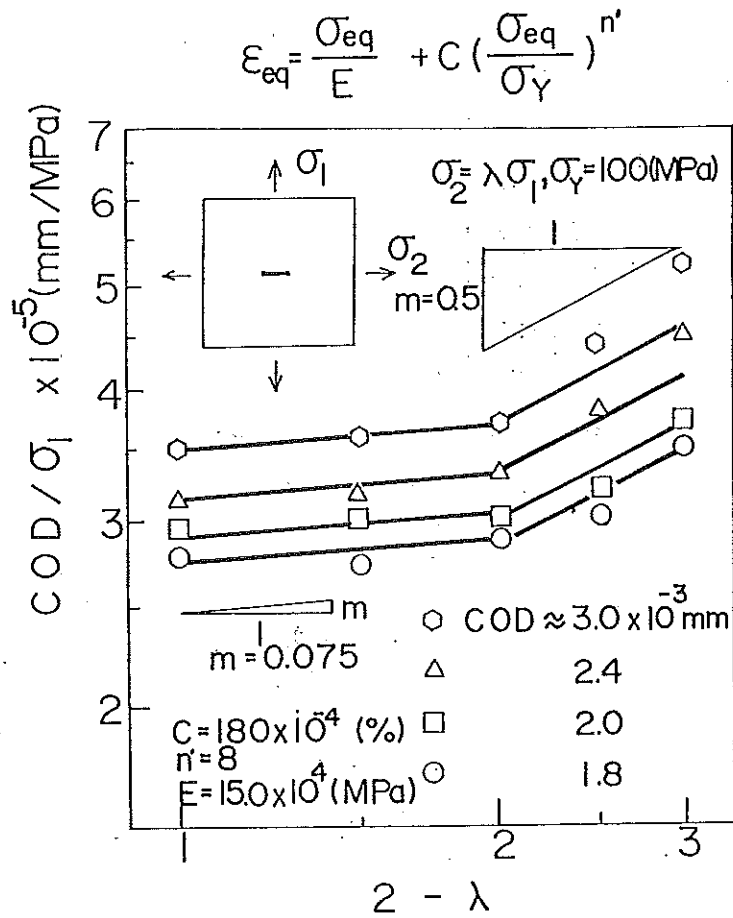


Fig.5 Relationship between crack opening displacement and principal stress ratio calculated from FEM.

the crack opening displacement and $(2-\lambda)$ in plane stress condition. The constitutive equation used is $\epsilon_{eq} = (\sigma_{eq}/E) + (\sigma_{eq}/\sigma_{eqy})^{n'}$, where ϵ_{eq} , σ_{eq} and σ_{eqy} are Mises' strain, Mises' stress and Mises' yield stress. The values of E, n' and C are respectively 1.5×10^4 MPa, 8 and 0.018% which are those of type 304 stainless steel at 873K [12]. The relationship between COD and $(2-\lambda)$ can be approximated by a straight line on log-log plotting and the slope of the line is 0.5 in the principal stress range of $2 < 2-\lambda < 3$ and 0.075 in $1 < 2-\lambda < 2$. The slope has almost a constant value in wide range of the constitutive relation from room temperature up to 923K [4] for type 304 stainless steel.

From holding the straight line, we can derive the equivalent stress, σ^* , which expresses the intensity of COD in biaxial stress state as;

$$\sigma^* = \alpha \sigma_1 (2-\lambda)^m, \quad (1)$$

where m is 0.5 in the range of $-1 < \lambda < 0$ and 0.075 in $0 < \lambda < 1$. Coefficient α is determined so that σ^* is reduced to σ_1 in the uniaxial stress state. The value of α is $1/\sqrt{2}$ in $-1 < \lambda < 0$ and 0.383 in $0 < \lambda < 1$. Equivalent strain ε^* , which corresponds to σ^* and expresses the intensity of COD, can be derived from the equivalent stress σ^* by continuum mechanics;

$$\varepsilon^* = \beta \varepsilon_1 (2-\phi)^{m'}, \quad (2)$$

β is 8.61 for $m' = -2.35$ in $-1 < \phi < 0$ and $\beta = 1.86$ for $m' = -0.25$ $0 < \phi < 1$. Figure 6 examines the relation of the stress and strain based multiaxial fatigue parameters normalized by the principal stress and strain. The COD stress is between the Mises and maximum principal stresses in $-1 < \lambda < 0$ and there is no large difference between all the parameters in $0 < \lambda < 1$, where σ_e is the equivalent stress proposed by Joshi [13]. On the strain base, the COD strain, as well as the γ^* -parameter [10] which is expressed as $(\gamma_{\max}^*/2) + 0.2\varepsilon_n^*$ increases as the principal strain ratio increases. The Mises' strain has the same trend as ε^* in the range of $-0.5 < \phi < 1$ but there exists contradiction in the range of $-1 < \phi < -0.5$. Figure 7[9] shows the experimental results in the principal strain controlled fatigue using a 1Cr-1Mo-1/4V steel cruciform specimen at 823K. The inverse of failure cycle corresponds to the failure parameter in Fig.6(b) so that the COD parameter and γ^* -parameter can be concluded to be a proper parameter.

4. Application of COD Criterion to Biaxial Fatigue Data.

Figure 8 [5] shows the correlation of the stress controlled data with σ^* which was derived in the previous section. The correlation of the data with σ^* is quite well. Figure 9 [7] correlates the strain controlled biaxial fatigue data with ε^* . The figure shows that the equivalent strain ε^* correlates well the push-pull, reversed torsion and combined push-pull/reversed torsion data. Although the transition of the fracture mode from mode I to mode II occurs at the principal strain ratio of 0.74, the correlation of the data with ε^* is in

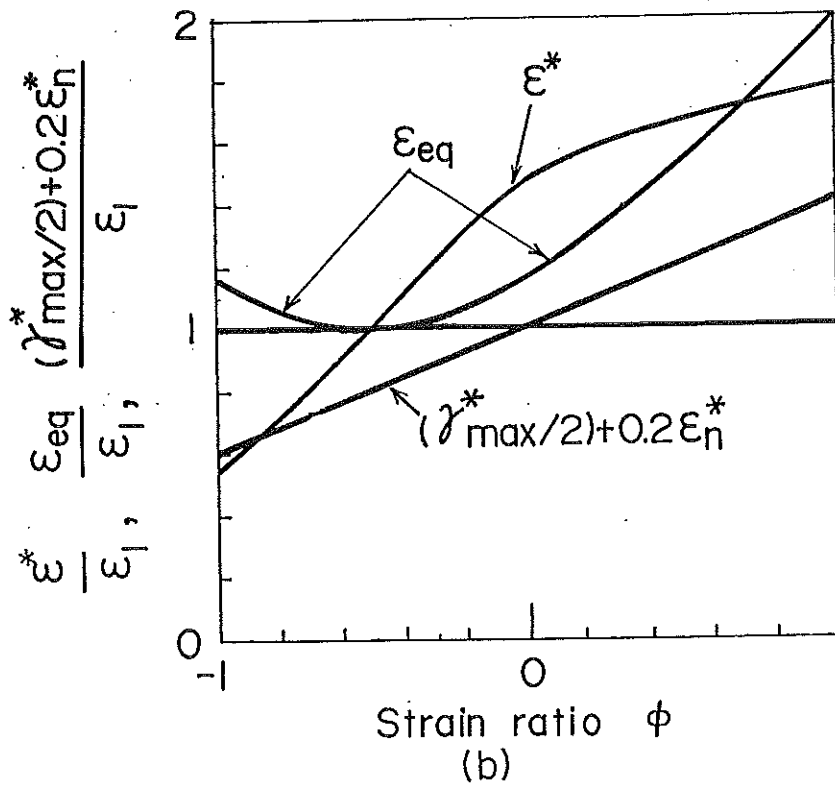
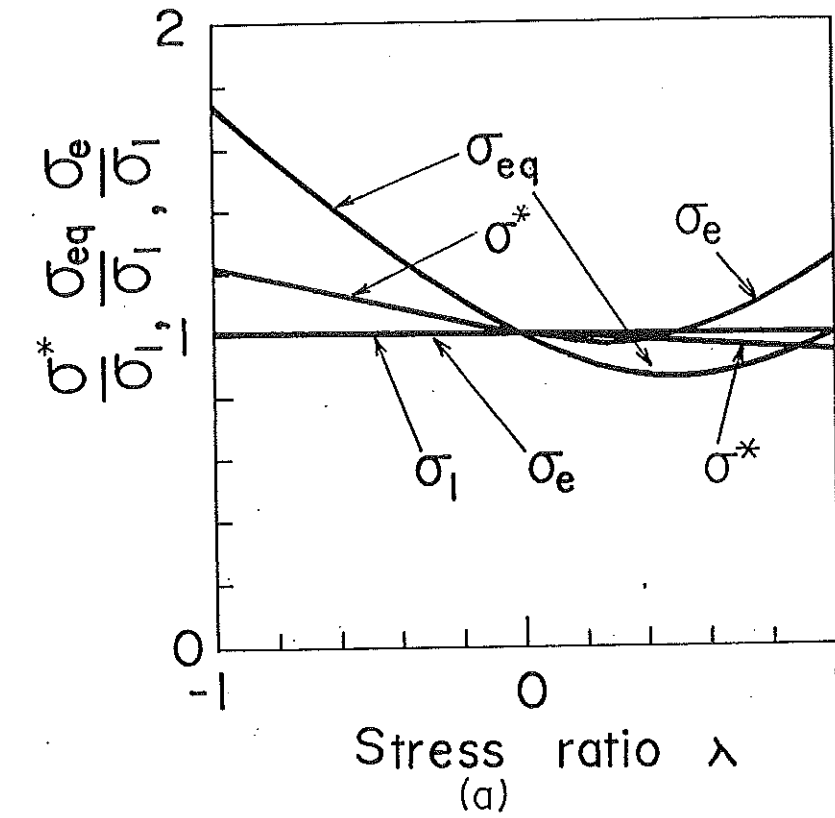


Fig.6 Comparison of COD parameter with other biaxial failure parameters.

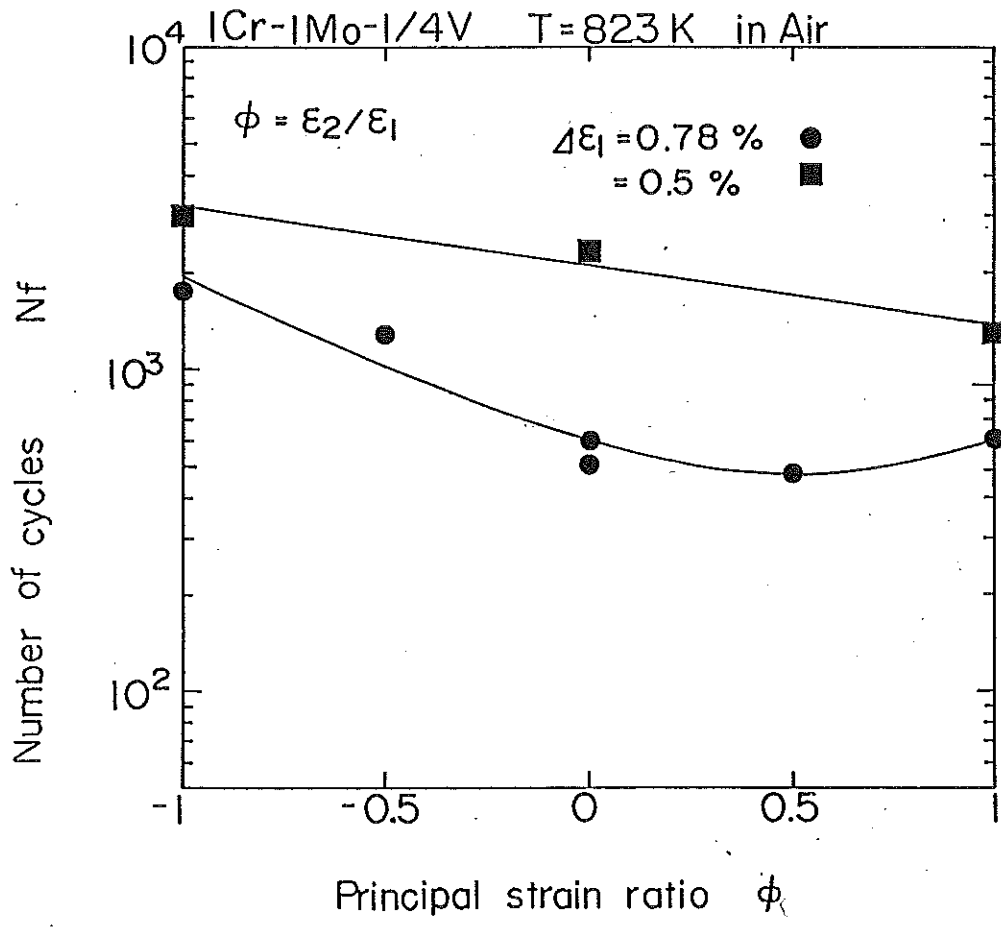


Fig.7 Biaxial fatigue life of 1Cr-1Mo-1/4V steel cruciform specimen in the principal strain range of $-1 < \phi < 1$ at 873K in air.

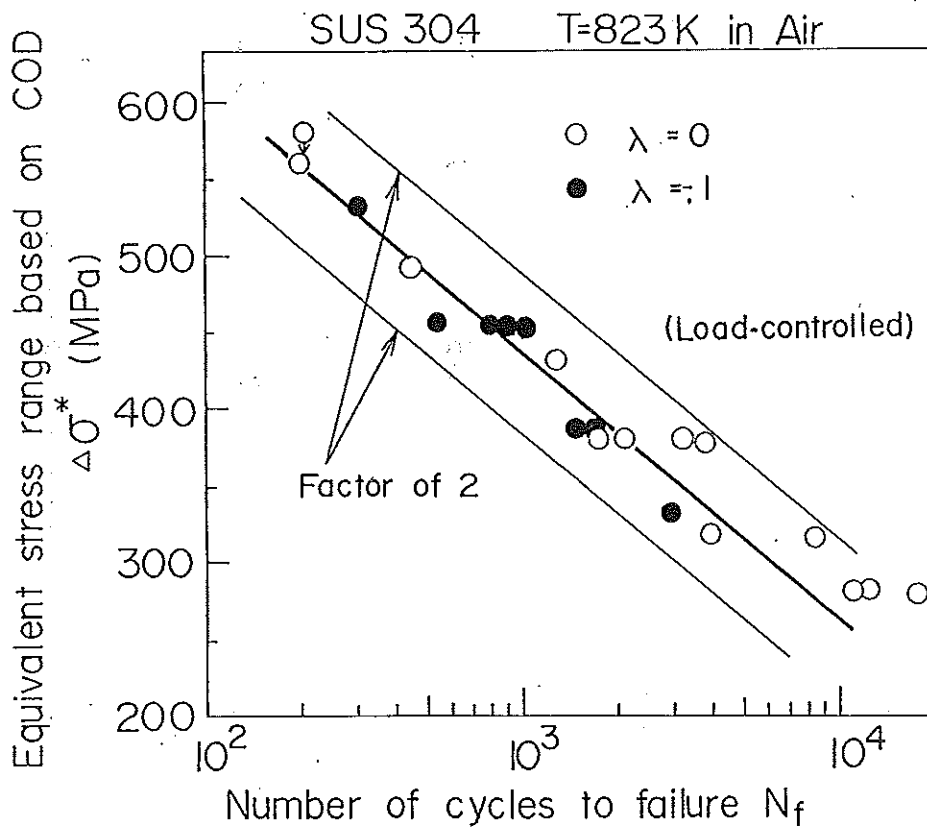


Fig.8 Correlation of the stress controlled biaxial fatigue data at 823K with σ^* .

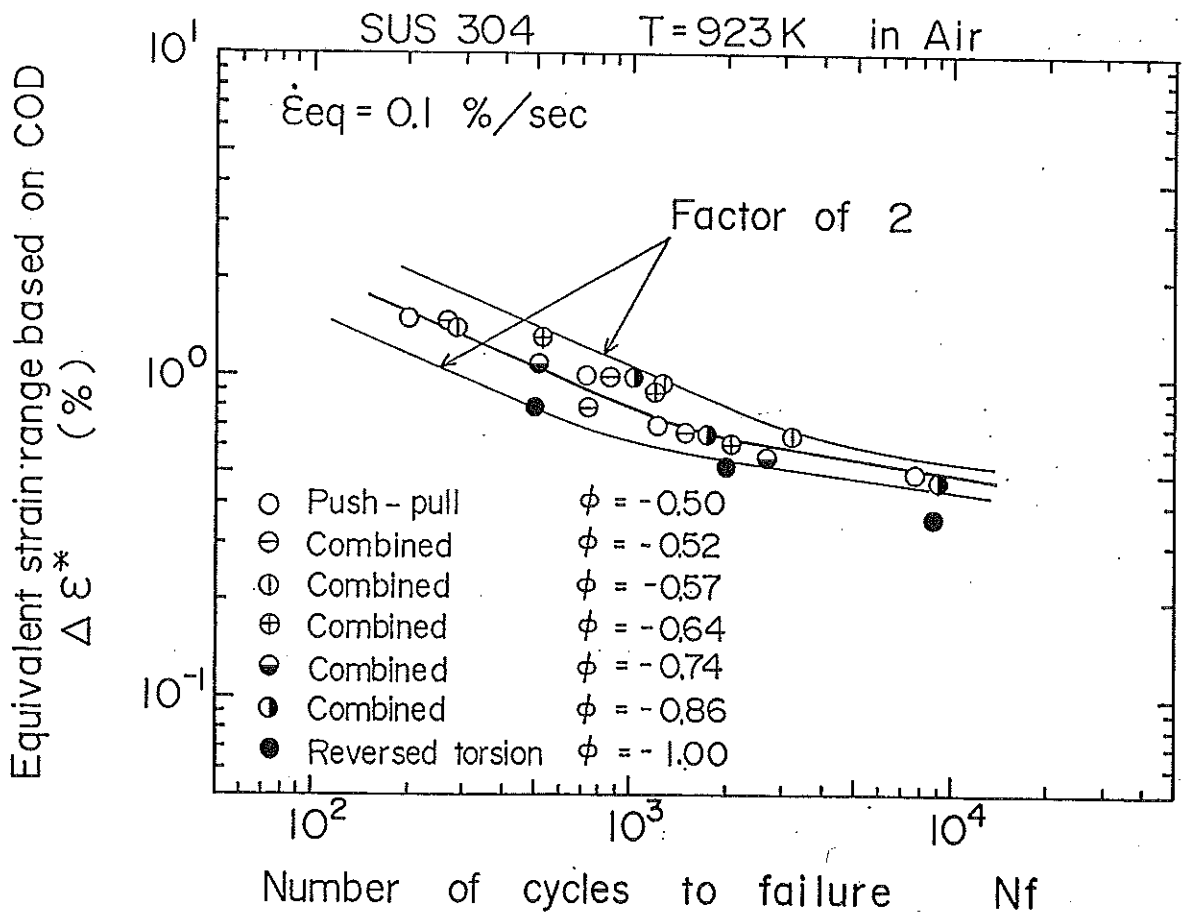


Fig.9 Correlation of the strain controlled biaxial fatigue data at 923K with ϵ^* .

success.

5. Conclusions

(1) The Mises' and maximum principal stresses are not a sufficient parameter to correlate the biaxial fatigue data. The cause of the unsuccessful data correlation is that both the stresses do not take account of the contribution of the parallel stress to the crack propagation properly.

(2) The COD stress and strain which take account of the parallel stress properly are derived. They are expressed as $\sigma^* = \alpha \sigma_1 (2 - \lambda)^m$ and $\varepsilon^* = \beta \varepsilon_1 (2 - \phi)^{m'}$. The material constants α , m , β and m' are $1/\sqrt{2}$, 0.5, 8.61 and -2.35 in the principal stress/strain ratio of $-1 < \lambda < 0$ and $-1 < \phi < 0$. They are 0.383, 0.075, 1.86 and -0.25 in the range of $0 < \lambda < 1$ and $0 < \phi < 1$.

(3) The COD stress and strain correlate successfully the stress and strain controlled biaxial low cycle fatigue data.

References

- [1] Ohnami, M. and Hamada, N., "Biaxial Low Cycle Fatigue of a SUS304 Stainless Steel at Elevated Temperature", Proc. of 25th Japan Congr. on Mater. Res., 1982, pp.93-99.
- [2] Hamada, N., Sakane, M., and Ohnami, M., "Creep Fatigue Studies under a Biaxial Stress State at Elevated Temperature", Fatigue of Engng. Mater. Struct., Vol.7, No.2, 1983, pp.85-96.
- [3] Ohnami, M., Sakane, M., and Hamada, N., "The Effect of Changing Principal Stress Axes on Low Cycle Fatigue Life in Various Strain Wave Shapes at Elevated Temperature", ASTM STP, 853, 1985, pp.622-634.
- [4] Hamada, N., Sakane, M., and Ohnami, M., "Effect of Temperature on Biaxial Low Cycle Fatigue Crack Propagation and Failure Life", Proc. of 30th Japan Congr. on Mater. Res., 1987, pp.69-75.
- [5] Hamada, N., Sakane, M., and Ohnami, M., "Study of High Temperature Low Cycle Fatigue Criterion in Biaxial Stress State", Bulletin of JSME, Vol.28, No.241,

1985, pp.1341-1342.

[6]Sakane, M., Ohnami, M., Nishino, S., and Hamada, N., "Low Cycle Fatigue and Constitutive Relation in Biaxial Stress State at Elevated Temperature", Inter. Conf. on Creep, JSME-IME-ASME-ASTM, Tokyo, Apr. 1986, pp.477-482.

[7]Sakane, M., Ohnami, M., and Sawada, M., "Fracture Mode and Low Cycle Fatigue Life in Biaxial Stress state at Elevated Temperature", ASME, J. Engng. Mater. and Tech., Vol.109, No.3, July, 1987, pp.236-243.

[8]Sakane, M., Ohnami, M., and Hamada, N., "Biaxial Low Cycle Fatigue for Notched, Cracked, and Smooth Specimens at High Temperature", ASME, J. Engng. Mater. and Tech., Vol.110, No.1, Jan., 1988, pp.48-54.

[9]Ohnami, M., Sakane, M., Nishino, S., and Itsumura, T., "Physical Mechanical Approaches to Cyclic Constitutive Relationships and Life Evaluation of Structural Materials in Biaxial Low cycle Fatigue at High Temperatures", Advanced Materials for Severe Service Applications, ed Iida, K. and McEvily, A.J., Elsevier Applied. Science, 1987, pp.165-182.

[10]Lohr, R.D. and Ellison, E.G., "A Simple Theory for Low-Cycle Multiaxial Fatigue", Fatigue Engng. Mater. Struct., Vol.3, No.1, Jan., 1980, pp.1-17.

[11]Kandil, F.A.; Brown, M.K. and Miller, K.J., "Biaxial Low-Cycle Fatigue Failure 316 Stainless Steel at Elevated Temperature", Mech. Behav. Nucl. Appl. Stainless Steel Elevated Temperature, 1982, pp.203-209.

[12] Cases of ASME Boiler and Pressure Vessel Code Case N-47, Class 1, Components in Elevated Temperature Service, Section 3, Division 1, the ASME (1978).

[13]Joshi, S.R. and Shewchuk, J., "Fatigue-Crack Propagation in Biaxial-Stress Fields", Exper. Mech., Vol.10, No.12, 1970, pp.529-533.